

CHAPTER 99

CIRCULAR CHANNEL BREAKWATER TO REDUCE WAVE OVERTOPPING AND ALLOW WATER EXCHANGE

Dal Soo LEE¹ Associate Member of ASCE,
Woo Sun PARK², and Nobuhisa KOBAYASHI³ Member of ASCE

Abstract

A new type of breakwater caisson is presented for improving water quality in a harbor. Circular resonance channels connected with flow conduits in the caisson cause clear sea water inflow into a harbor through the conduits. The hydraulic characteristics of this caisson with respect to wave reflection, overtopping and transmission appear excellent compared with those of conventional caissons. The potential of water quality improvement is great due to its high efficiency in normal wave conditions. A simple resonance model is developed to identify an important dimensionless parameter. Experimental results show that the new concept of circular channel breakwater is promising in terms of its hydraulic performance.

Introduction

The main function of existing breakwaters is to reduce waves propagating onshore, and for normal wave conditions, the breakwaters are designed for no wave overtopping to secure harbor tranquility. However, it is normally overlooked that the breakwaters usually block sea water exchange at the cost of the harbor

¹Principal Res. Engr., Director of Ocean Engrg. Div., Korea Ocean Res. & Dev. Inst., Ansan P.O.Box 29, Seoul 425-600, Korea.

²Senior Res. Engr., Ocean Engrg., Div., Korea Ocean Res. & Dev. Inst., Ansan P.O.Box 29, Seoul 425-600, Korea

³Professor and Associate Director, Center for Applied Coastal Research, University of Delaware, Newark, Delaware 19716, USA

tranquility. This often causes water pollution problems due to the stagnation of sea water inside the harbors if tidal ranges are not sufficiently large.

Several kinds of breakwaters have already been developed to allow water exchange (Kataoka and Saida, 1986; Tanimoto et. al, 1987; Korea Ocean Research and Development Institute, 1989; Tanimoto et. al, 1989), but most of them are normally effective only in the presence of currents. No breakwater type with water quality improving capability mainly under weak wave action appears to exist at the present. Hence, there is a practical need to develop a breakwater type that causes clear sea water inflow into a harbor through the breakwater using incoming waves as a driving force. In addition, the performance of the breakwater with respect to wave reflection, overtopping and transmission should be improved as much as possible.

The circular channel breakwater(CCB) equipped with flow conduits presented herein has been devised to attain the capability of wave-induced sea water inflow into a harbor as well as low wave reflection and overtopping at the same time. The resonance phenomena of water level in the circular channel is shown to be important in increasing water flow rates for short period waves. A simple resonance model is developed to identify an important dimensionless parameter for the analysis of experimental data. Experimental results show that the concept of CCB is promising.

Conceptual Description of CCB

Figure 1 shows a conceptual diagram of the Circular Channel Breakwater(CCB). The caisson has circular channels at its front part and flow conduits at its rear part. When incident waves impinge on the CCB, water passes through the channel. Water inflow into a harbor occurs through the conduits due to the pressure difference between the inlet and outlet of these conduits. The inflow induces a small rise of mean water level behind the breakwater, and the pressure driven weak current is subsequently introduced into the harbor but occurs essentially continuously under normal wave conditions. A reverse flow is restricted because the inlets of the conduits are placed near the still water level in the circular channels to create one way flow into the harbor.

The water inflow does not make any significant disturbance of water surface in the harbor under normal wave conditions because

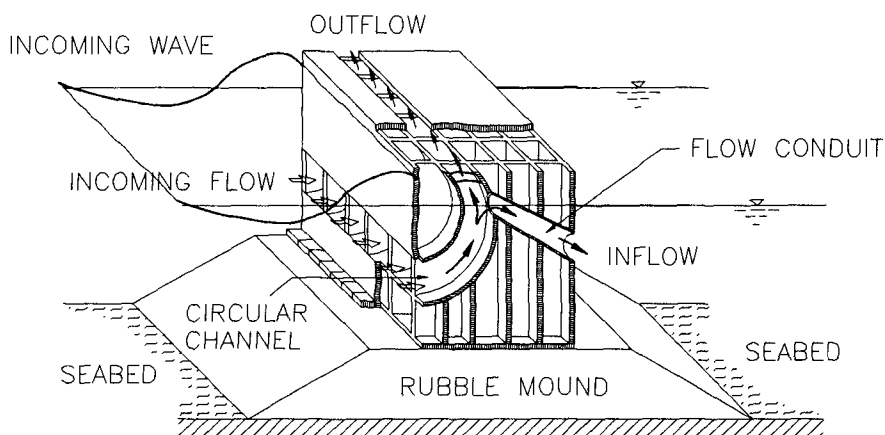


Figure 1. Conceptual diagram of the Circular Channel Breakwater (CCB).

the outlet of the conduits are well submerged. The back face of the caisson may be used as a wharf for small ships under moderate wave conditions when the outlets of the conduits are placed well below the draft of a ship.

Resonant oscillations occur in the circular channel for short period waves and hence enhance the flow rate. On the other hand, when wave overtopping occurs, the outflow issuing from the circular channel collides with the overtopping water flow above the caisson, resulting in increased wave energy dissipation and reduced wave overtopping.

Simple Resonance Model

A simple resonance model is developed to gain insight into the complicated hydrodynamic process in the circular channel and to identify an important dimensionless parameter for the following experimental data analysis.

Figure 2 shows the geometric parameters and cylindrical coordinate system(r, θ) used in the following linear potential flow analysis, where R_c and b are the circular channel radius and its width, respectively, $\eta_c(t)$ is the free surface elevation in the channel, θ_s is the value of θ at still water level in the channel,

$P_e(t)$ is the pressure at the channel entrance, and d is the water depth. It is assumed that the circular channel radius R_c is much larger than its width b , and that no overflow occurs from the exit of the channel.

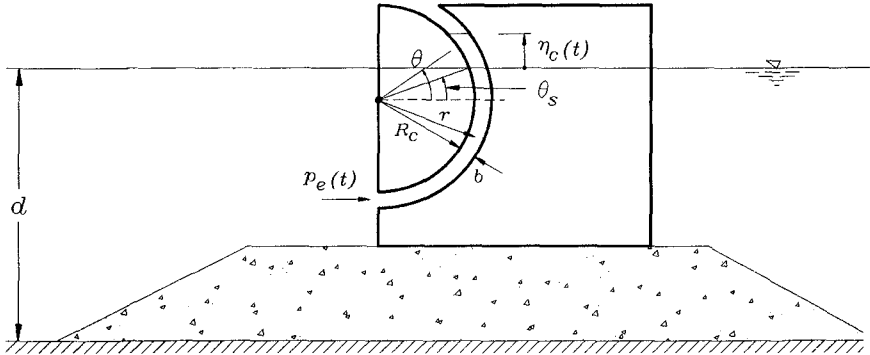


Figure 2. Diagram showing geometric parameters in cylindrical coordinate system.

The Laplace equation for the velocity potential ϕ in the circular channel is expressed as

$$\frac{1}{r} \frac{\partial}{\partial r} \left(r \frac{\partial \phi}{\partial r} \right) + \frac{1}{r^2} \frac{\partial^2 \phi}{\partial \theta^2} = 0 \quad (1)$$

The boundary conditions may be expressed as

$$-\rho \frac{\partial \phi}{\partial t} = P_e(t) \quad \text{at } \theta = -\frac{\pi}{2} \quad (2)$$

$$\frac{\partial \eta_c}{\partial t} = \frac{1}{R_c} \frac{\partial \phi}{\partial \theta} \cos \theta_s \quad \text{at } \theta = \theta_s \quad (3)$$

$$-\frac{\partial \phi}{\partial t} = -g\eta_c \quad \text{at } \theta = \theta_s \quad (4)$$

$$\frac{\partial \phi}{\partial r} = 0 \quad \text{at } r = R_c \quad \text{and} \quad r = (R_c + b) \quad (5)$$

where, $\phi(r, \theta, t)$ = velocity potential inside the circular channel
 $P_e(t)$ = dynamic pressure at the entrance of the channel
 as shown in Figure 2
 ρ = water density
 η_c = free surface elevation in the channel
 θ_s = value of θ at the still water level in the channel

Equations (3) and (4) correspond to the linearized kinematic and dynamic free surface boundary conditions.

To satisfy the no flux boundary condition on the curved solid walls given by Equation (5), the solution ϕ of Equation (1) should be independent of r as

$$\phi(\theta, t) = C_1(t)\theta + C_2(t) \quad (6)$$

Using Equation (3),

$$C_1(t) = \frac{R_c}{\cos \theta_s} \frac{\partial \eta_c}{\partial t} \quad (7)$$

From Equations (2) and (4),

$$\frac{dC_1(t)}{dt} \left(-\frac{\pi}{2}\right) + \frac{dC_2(t)}{dt} = -\frac{1}{\rho} P_e(t) \quad (8)$$

$$\frac{dC_1(t)}{dt} \theta_s + \frac{dC_2(t)}{dt} = -g\eta_c \quad (9)$$

Eliminating $C_1(t)$ and $C_2(t)$ from Equations (7), (8) and (9), we get

$$\frac{R_c(\theta_s + \frac{\pi}{2})}{\cos \theta_s} \frac{d^2 \eta_c}{dt^2} + g\eta_c = \frac{1}{\rho} P_e(t) \quad (10)$$

which indicates the free surface oscillation in the channel forced by the dynamic pressure $P_e(t)$ at the channel entrance.

Assuming simple harmonic motions for $\eta_c(t)$ and $P_e(t)$ expressed as

$$\eta_c(t) = R_e[\bar{\eta}_c e^{-i\omega t}] \quad (11)$$

$$P_e(t) = R_e[\bar{P}_e e^{-i\omega t}] \quad (12)$$

where R_e indicates the real part, $\bar{\eta}_c$ and \bar{P}_e are the complex valued amplitudes, and ω is the angular frequency. Substituting Equations (11) and (12) into (10) yields :

$$\bar{\eta}_c = \left[1 - \frac{R_c(\theta_s + \frac{\pi}{2})\omega^2}{g \cos \theta_s} \right]^{-1} \cdot \frac{1}{\rho g} \bar{P}_e \quad (13)$$

In order to find \bar{P}_e , the solution in the channel will need to be matched with the solution in front of the caisson. Nevertheless, this simple solution indicates that resonance occurs in the circular channel when,

$$\frac{R_c(\theta_s + \frac{\pi}{2})\omega^2}{g \cos \theta_s} = 1 \text{ for infinite } \eta_c.$$

In reality, η_c will not be infinite due to energy loss especially at the channel entrance.

For the following data analysis the dimensionless parameter ω^* is defined as

$$\omega^* \equiv \frac{R_c(\theta_s + \frac{\pi}{2})\omega^2}{g \cos \theta_s} \quad (14)$$

where $\omega^* = 1$ corresponds to the resonance condition.

Experiments and Data Analyses

Experiments on the circular channel breakwaters(CCB) were conducted to examine the hydrodynamic characteristics of wave reflection, overtopping, transmission and water discharge through the flow conduits. The experiments were performed with regular waves in a wave flume (53.3 m long, 1.0 m wide, and 1.25 m high)

with a model caisson as shown in Figure 3, where the water depth on the horizontal bottom is $d=40.5\text{ cm}$, the caisson crest height above the still water level is $h_c=8.5\text{ cm}$, the radius of the front wall of the channel is $r_{c1}=8.5\text{ cm}$, the radius of the rear wall of the channel is $r_{c2}=15\text{ cm}$, the width of the channel at the entrance is $b_e=10\text{ cm}$, and the diameter of the flow conduit is $D=3.2\text{ cm}$. The incident wave height H_i was 3 and 5 cm in these experiments. In this model the channel width was designed to be decreased gradually upward to produce higher runup inside the channel. Additional experiments were also carried out for the solid wall breakwater (SWB, conventional caisson breakwater) for the purpose of comparisons.

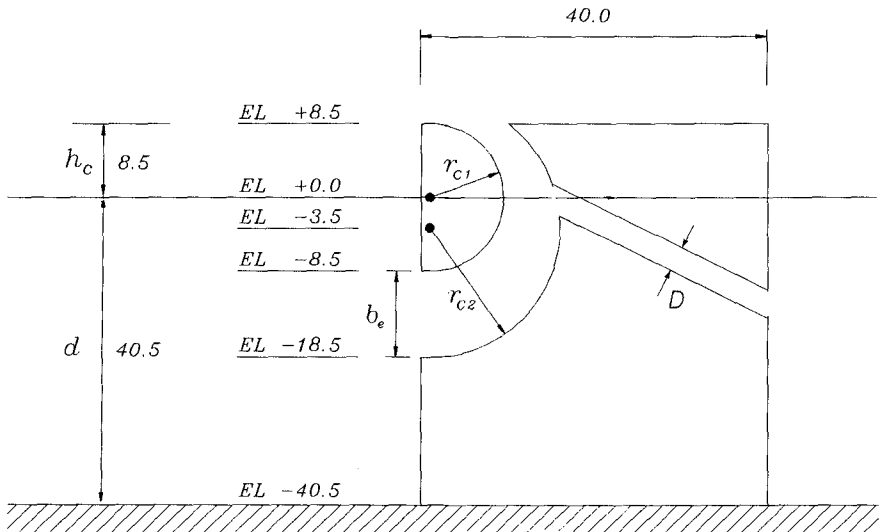


Figure 3. Cross-sectional diagram of model setup without rubble mound foundation(unit : cm).

Figure 4 shows the measured wave runup $\eta_{c\text{ max}}$ inside the channel normalized by the incident wave height H_i as a function of ω^* defined by (14). Comparing the measured values of $\eta_{c\text{ max}}/H_i$ with the value of 1.0 in front of a perfectly reflective vertical wall, this runup in the vicinity of $\omega^*=1$ serves as an amplified potential

for driving inflow into the harbor through the flow conduits.

The occurrence of the peak at the resonance frequency (at the value of $\omega^*=1$ in Figure 4) means that the resonance plays a major role in the enhancement of runup in the channel. In shelter coastal areas, the waves of short periods and small wave heights prevail, as a result, the energy of normal waves can be effectively used to induce water inflow into a harbor by the use of this type of breakwater.

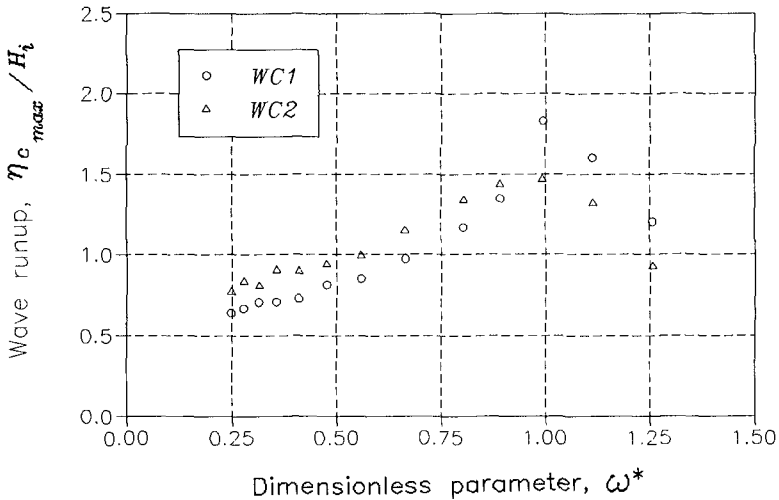


Figure 4. Maximum wave runup inside the circular channel shown in Figure 3 for $H_i=3cm$ (WC1) and $H_i=5cm$ (WC2).

Figure 5 shows that the reflection of the CCB is lower than that of the SWB. The occurrence of the lowest reflection near the resonance frequency (near the value of $\omega^*=1$ in Figure 5) means that the resonance reduces significantly reflection from CCB. The resonance peak in this figure is shifted to slightly higher frequency for the tests with $H_i=3cm$.

Figure 6 shows the measured net flow rate Q normalized by $\sqrt{2gH_i}A$ with g =gravitational acceleration and $A=(\pi/4)D^2$ through one flow conduit of diameter $D=3.2cm$ for the model caisson shown in Figure 3. The resonant peak in this figure is shifted to slightly lower frequency for the tests with $H_i=5cm$.

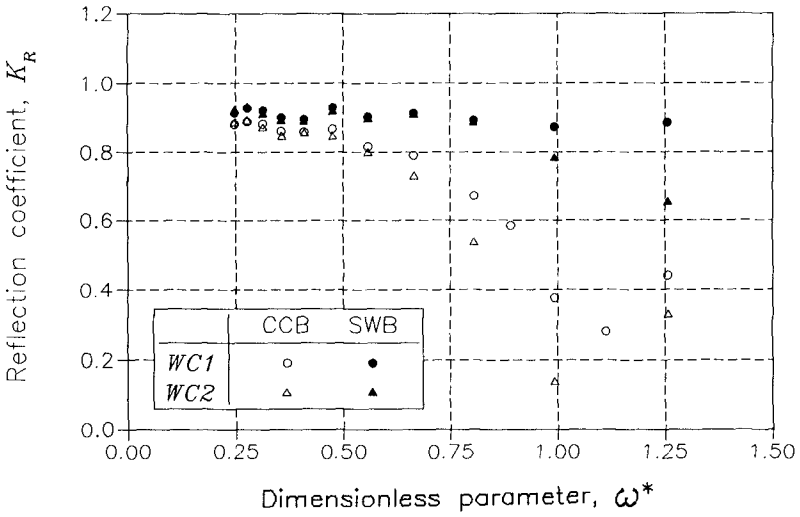


Figure 5. Comparison of reflection coefficients between CCB shown in Figure 3 and SWB for $H_i=3cm$ (WC1) and $H_i=5cm$ (WC2).

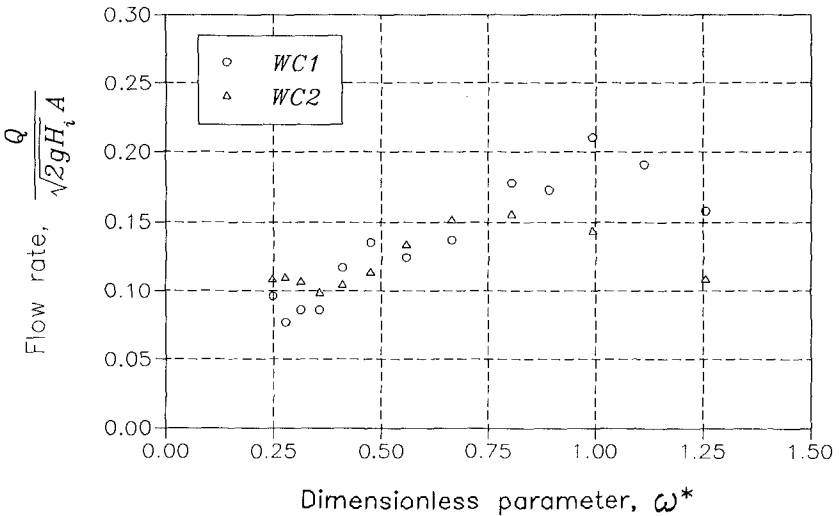


Figure 6. Net inflow rate through one flow conduit with $D=3.2cm$ for $H_i=3cm$ (WC1) and $H_i=5cm$ (WC2).

Figures 7 and 8 show model setup with a rubble mound and the different positions ($C1$, $C2$ and $C3$) of flow conduit inlets in the circular channel, respectively. The crest elevation h_c above the still water level was chosen as 12 cm and 8 cm by changing the water depth in the tank. In Figures 7 and 8, $h_c=12\text{ cm}$, while the water depths on the bottom and above the foundation are $d=50\text{ cm}$ and $h=30\text{ cm}$:

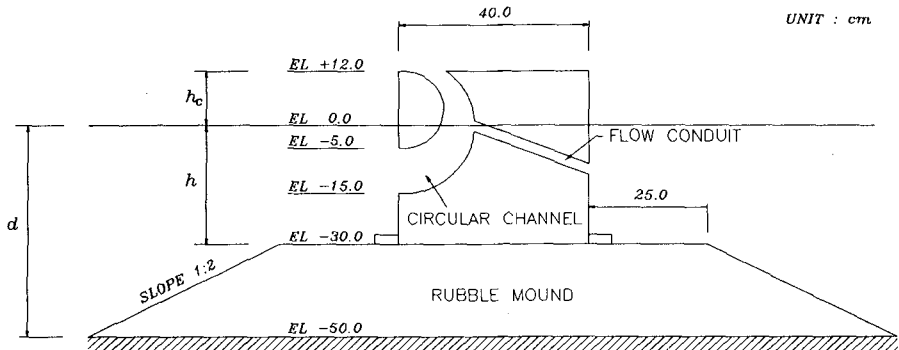


Figure 7. Cross-sectional diagram of model setup with rubble mound foundation.

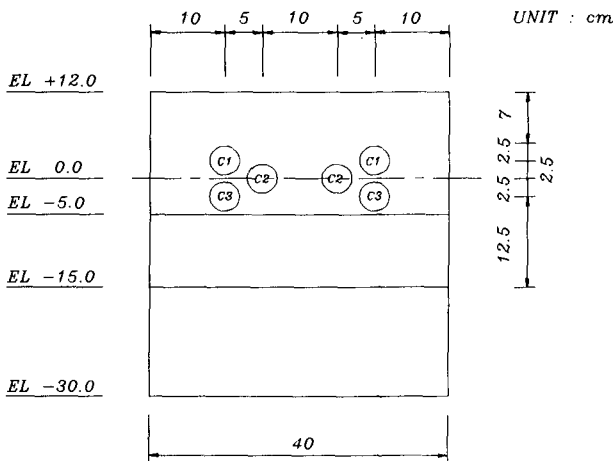


Figure 8. Schematic diagram showing different positions ($C1$, $C2$ and $C3$) of flow conduit inlets in the circular channel in Figure 7.

Only some of the many geometric parameters involved in the caisson were changed. It should therefore be noted that the experimental results presented hereafter are not general and limited to the adopted model configuration and experimental conditions. For the experimental setup shown in Figure 7 wave overtopping occurred for the incident wave height $H_i=13\text{ cm}$ and the simple model discussed in the previous section is not applicable.

Figure 9 shows the comparison of the net flow rate Q through one conduit of diameter $D=3.2\text{ cm}$ where l is the length of the flow conduit. At position C3 (below the still water level), the net flow rate is generally low for the longer period waves due to the occurrence of reverse flow in the conduit under the minimum free surface elevation in the channel. At position C1 (above the still water level), the net flow rate is generally low for shorter period waves due to the short duration of the head difference between the inlet and outlet of the flow conduit. At position C2 (at the still water level) the net flow rate remains to be large for any wave period. The variation pattern of the net flow rate with respect to the inlet position may vary if the configuration of the channel is changed.

Figure 10 shows that the reflection from the CCB is lower for all frequencies than that from the SWB. The relative difference increases with the increase of $\omega^2 d/g$. This means that CCB retains the merit of low reflection of perforated wall caisson breakwaters.

Figures 11 and 12 show measured values of overtopping rate and transmission coefficient for the water depth condition different from that shown in Figure 7. The caisson crest height above the still water level is $h_c=8\text{ cm}$, and the water depths on the bottom and above the foundation are $d=54\text{ cm}$ and $h=34\text{ cm}$, respectively. Figure 11 shows that the overtopping rate q of CCB per unit width is always lower than that of SWB. This means that the outflow issuing from the exit of the circular channel plays an important role in reducing wave overtopping due to its collision with the landward overtopping water above the caisson. Figure 12 shows the resulting difference in the wave transmission coefficient between CCB and SWB.

The characteristics of low reflection together with low

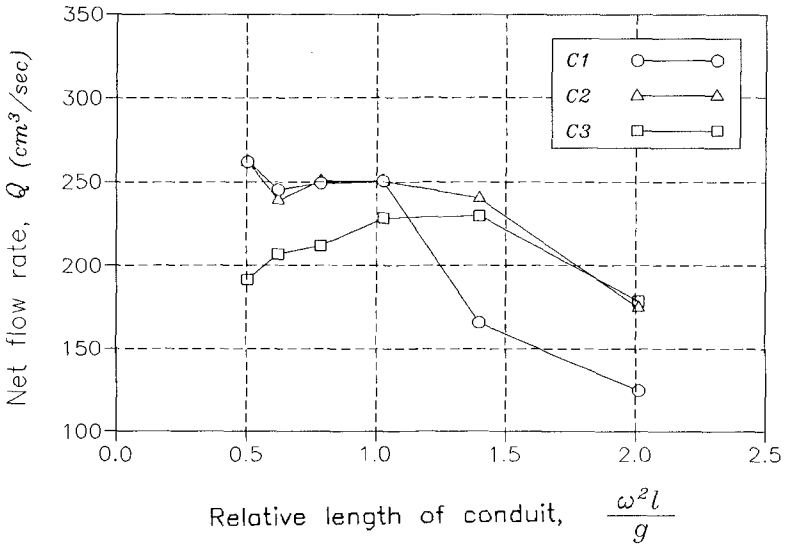


Figure 9. Variations of net inflow rate Q through one flow conduit in Figure 8 with $d=50\text{ cm}$, $h=30\text{ cm}$, $h_c=12\text{ cm}$ and $D=3.2\text{ cm}$ for $H_i=13\text{ cm}$.

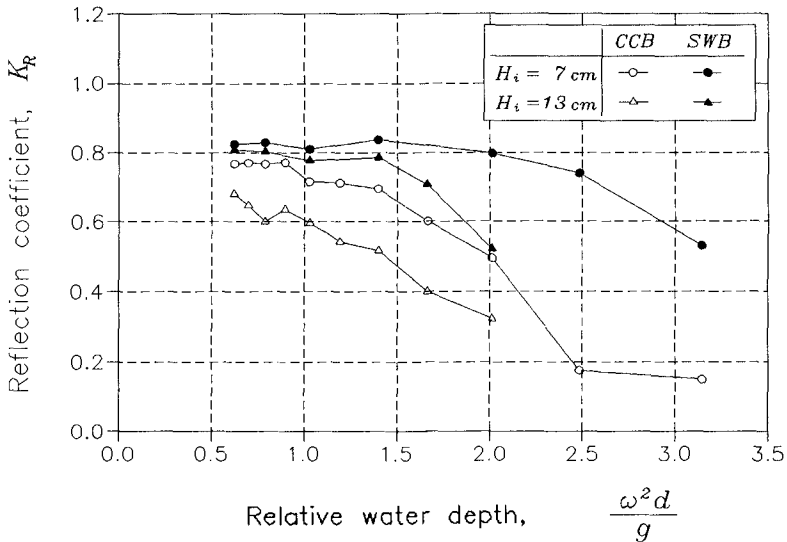


Figure 10. Comparison of reflection coefficients between CCB and SWB with $d=50\text{ cm}$, $h=30\text{ cm}$, $h_c=12\text{ cm}$ in Figure 7 for $H_i=7$ and 13 cm .

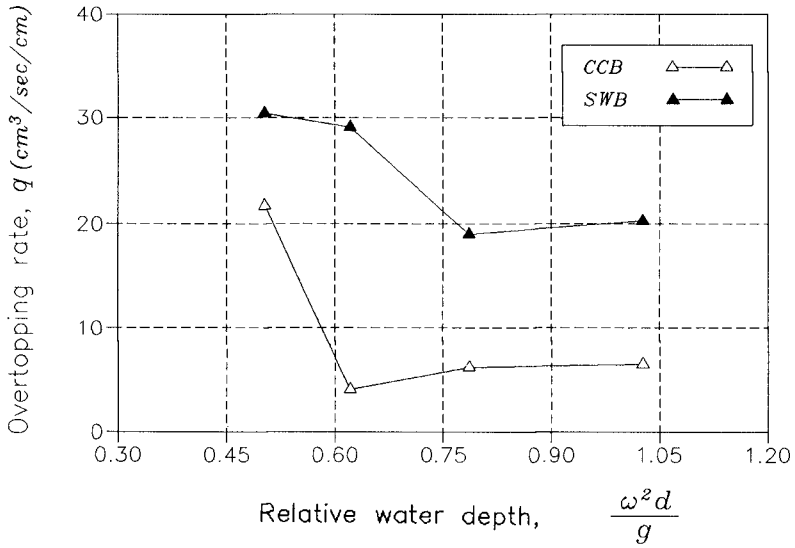


Figure 11. Comparison of overtopping rates between CCB and SWB with $d=54\text{ cm}$, $h=34\text{ cm}$ and $h_c=8\text{ cm}$ in Figure 7 for $H_i=13\text{ cm}$.

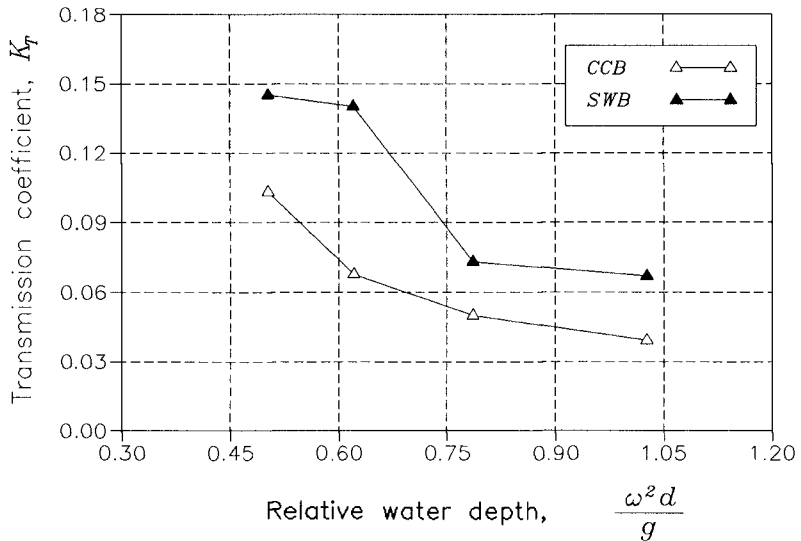


Figure 12. Comparison of transmission coefficients between CCB and SWB with $d=54\text{ cm}$, $h=34\text{ cm}$ and $h_c=8\text{ cm}$ in Figure 7 for $H_i=13\text{ cm}$.

transmission imply that the hydraulic performance of CCB is superior to that of SWB.

Conclusions

A circular channel breakwater (CCB) connected with flow conduits was proposed. The performance of CCB in terms of wave reflection, overtopping and transmission is excellent compared with that of conventional solid wall caisson breakwaters.

The capability of inducing clear water inflow through the conduits of CCB into a harbor is enhanced by the resonant oscillations in the circular channel under normal wave conditions. A great potential for improving water quality in harbors is expected under normal wave conditions when water quality problems may become serious. At the same time, CCB maintains the merits of caisson type breakwaters in that the upper and back faces of the caisson can be utilized.

Further studies are needed to reveal the dynamic characteristics related to the pressure distribution and resulting caisson stability.

Acknowledgements

The present study was financially supported by the Ministry of Science and Technology of Korea through the Project No. BSPN 00232.

References

- Kataoka, S. and Saida, K. (1986). Compilation of Breakwater Structure, Technical Note of the Port and Harbour Research Institute, Ministry of Transport, Japan, No. 556 (in Japanese).
- Korea Ocean Research and Development Institute, (1989). A Study on the Development of New Coastal Structures for Wave Absorption (I), BSPG 00077-224-2 (in Korean).
- Tanimoto K., Namerikawa, N., Ishimaru, Y. and Sekimoto, T. (1987). Hydraulic Characteristics and Design Wave Forces of Double-cylindrical Caisson - A Study on Development of Deep-water Breakwater, Technical Note of the Port and Harbour Research Institute, Ministry of Transport, Japan, No.

600 (in Japanese).

Tanimoto K., Kataoka, S., Haranaka, S., Suzuki, S., Shimosako, K. and Miyazaki, K. (1989). A Hydraulic Experimental Study on Semi-circular Caisson Breakwaters, Technical Report of the Port and Harbour Research Institute, Ministry of Transport, Japan, Vol. 28, No. 2 (in Japanese).